

IMPERIAL COLLEGE LONDON

DEPARTMENT OF ELECTRICAL AND ELECTRONIC ENGINEERING

Structure and dynamics of large networks of interacting neurons

Author:

Alejandro Gilson Campillo

CID:

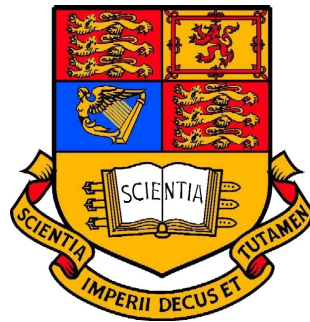
01112712

Supervisor:

Prof. Pier Luigi Dragotti

Second marker:

Dr. Wei Dai



A thesis submitted for the degree of

MEng Electrical and Electronic Engineering

June 4, 2019

Abstract

This project tries to understand how real biological neural networks are connected by treating the system as a diffusion process. By selecting the connectivity weights of each of the neurons that maximize the likelihood of some recorded spikes occurring the structure of the network is estimated. For this project, the speed and scalability of NetRate (the implemented algorithm) is improved and its constraints are analysed. Moreover, the model of neural network and inference algorithm are changed for it to be used on a real mouse's spike data-set and a benchmark is presented for analysing inference accuracy when no ground truth is available.

Acknowledgements

It is usual to thank those individuals who have provided particularly useful assistance, technical or otherwise, during your project.

Contents

1	Introduction	6
2	Background	7
2.1	Definition of connectivity	7
2.2	Izhikevich neuron model	8
2.3	Netrate	9
2.3.1	Diffusion processes	9
2.3.2	Mathematical definitions	10
2.3.3	Derivation of NetRate	11
2.3.4	Cascade generation	13
2.3.5	Performance metrics	14
2.4	Biological Neural Network	14
2.4.1	Structure of the Network	14
2.4.2	Input stimulus model for cascade generation	15
2.4.3	Likelihood function	16
2.4.4	Network inference results	17
3	Improving the speed of NetRate	18
3.0.1	Parallelization of NetRate	19
3.0.2	Speed improvement results	21
4	Simulating a biological neural network	24
4.1	Mouse somatosensory cortex neuron dataset	25
4.2	Input stimulus to the system	25
4.2.1	System with random spikes	26
4.3	Number of spikes	27
4.4	Cascade generation	28
4.4.1	Method of maximum cascades	29
4.4.2	Method of maximum independence	29
4.4.3	Optimal cascade generation	29
4.5	Concluding remarks	29

5	Inferring the connectivity of a mouse's neuronal system	30
5.1	Evaluating the performance without a ground truth	30
5.2	Results	30
6	Conclusion	31

List of Figures

2.1	Types of neurons in the mammalian brain. Generated with the Brian Simulator [7] using the Izhikevich neuron model [6]	9
2.2	Adjacency matrix of a network of 20 nodes	15
3.1	Diagram of the NetRate parallelization process	20
3.2	Computation time of NetRate	22
4.1	Histogram of the number of spikes in a network of 98 neurons	26
4.2	Number of spikes as a function of the parameter I for a 1 hour simulated network of 98 neurons and a random spike stimulus	27

List of Tables

2.1	Results for network inference obtained in [4]	17
4.1	Spike characteristics of different types of neural networks	28

Chapter 1

Introduction

The brain is a complex machine, it allows the human being to think, communicate and feel. It does so thanks to the billions of neurons that communicate in a dense network through synapses. However, little is known about how it works. By studying how the neurons structure to store and process information we can understand how the brain as a whole functions. This could have important applications in medicine for curing diseases such as Parkinson [1] and epilepsy [2], and in machine learning for the development of more intelligent neural networks.

In order to infer the network structure of a set of neurons, they are treated as a diffusion network where electrical spikes increase the likelihood of connected neurons to spike and therefore transmit a signal that travels as if it were a disease. By evaluating the time of "infection", the relationship between two neurons can be probabilistically estimated. After computing the relationship between all of the neurons, an estimate of the topology of the network can be obtained.

Previous work on this topic [3, 4] evaluated the feasibility of using a maximum-likelihood estimator algorithm, NetRate [5], for the inference of the structure of biological neural networks. A network was simulated using the Izhikevic neuron model [6] and the Brian simulator [7]. The connections between the neurons were then estimated, compared to the original network and the performance of the algorithm was evaluated. Recent developments in technology now allow scientists to obtain individual neuron spike information from the brain tissue [8, 9, 10]. This data is very useful and serves as a mean of evaluating the performance of the algorithm with real neurons. Moreover, this information can help in creating simulated networks that resemble more the real biological ones.

Chapter 2

Background

2.1 Definition of connectivity

The definition of connectivity between neurons has a history of lack of consensus among the scientific community. Connectivity studies from different researchers may lead to different results depending on how they define it, as they may be looking at different aspects of connectivity. The two main accepted definitions that are used are functional and effective connectivity [11].

Functional connectivity is the temporal correlation between spatially remote neurophysiological events [12]. Studies on this topic began with electroencephalography (EEG) measurements. Some methods to measure functional connectivity include the evaluation of the correlation in the frequency domain between EEG signals at different scalp locations [13], and the cross-correlation of the time series measurements from a pair of electrodes [14]. However, due to the volume conduction of brain tissue, the electrical activity from the scalp cannot infer the individual neuron behaviour below the electrode [11].

Effective connectivity was defined in [12] as the influence that one neural system exerts on another. Effective connectivity can be measured in terms of efficacy and contribution. At a synaptic level it can be expressed as in Eq.2.1, where x_j is the post-synaptic response to many pre-synaptic inputs x_i and \mathbf{W}_{ij} is the efficacy of the connections between neurons i and j . Contribution is reflected in Eq.2.2 as the effect of i on j relative to all pre-synaptic inputs. Using this definition, directional effects are taken into account and a richer representation of the network can be attained. Following the approach in [4], this project will focus on the effective connectivity of neurons in a network.

$$x_j = \sum \mathbf{W}_{ij} \times x_i \quad (2.1)$$

$$\frac{\mathbf{W}_{ij}}{\sum \mathbf{W}_{ij}} \quad (2.2)$$

2.2 Izhikevich neuron model

In order to understand how the brain works we must be able to replicate the behaviour of individual neurons applying simple and accurate models. However, as explained in [6], meeting both criteria can be challenging. The Hodgkin–Huxley model [15] is very accurate as it can emulate the rich firing patterns of many types of neurons. However, it is very computationally expensive and only a few neurons can be computed in real time. The integrate-and-fire model [16] has the opposite problem: it is computationally simple but it is an unrealistic representation of the neuron since it does not capture the firing patterns with sufficient accuracy [6]. In contrast, the Izhikevich neuron model [6] meets both criteria. Tens of thousands of spiking cortical neurons can be simulated in real time by simplifying the Hodgkin-Huxley model into the two dimensional system of differential equations shown below.

$$v' = 0.04v^2 + 5v + 140 - u + I \quad (2.3)$$

$$u' = a(bv - u) \quad (2.4)$$

with the auxiliary after-spike resetting

$$\text{if } v \geq 30\text{mV, then } \begin{cases} v \leftarrow c \\ u \leftarrow u + d \end{cases} \quad (2.5)$$

Here, the dimensionless variables v and u represent the membrane potential of the neuron and the membrane recovery, respectively. When a spike reaches its apex (30 mV), both these variables are reset according to Eq. 2.5. The differentiation is taken with respect to time. Synaptic or injected DC currents are represented by the variable I . Just as with real neurons, the threshold is not fixed and it's based on previous spikes.

On the other hand, a, b, c and d are dimensionless parameters. a determines the speed of the recovery variable u , b defines the sensitivity of the recovery variable u to sub-threshold fluctuations of the membrane potential v . Finally, c and d determine the after-spike reset value of the recovery variables v and u , respectively.

The relevance of this algorithm stems from the fact that, different combinations of the parameters provide the model with a rich variety of firing patterns. When analysing the neocortical neurons in the mammalian brain, a number of different classes of excitatory neurons can be found [17, 18] such as RS (regular spiking), IB (intrinsically bursting) and CH (chattering). From the inhibitory type of neurons, two classes can be found: FS (fast spiking) and LTS (low-threshold spiking). Other interesting classes of neurons are the TC (thalamo-cortical) and the RZ (resonator). A visual representation of these neurons can be observed in figure 2.1. It is of great importance to understand what types of neurons can be found so that a simulated network can become a closer representation of what can be found on a real brain. In order to simplify the network to be inferred, the only type of neurons simulated in the network were the excitatory regular spiking neurons. This was achieved by setting the parameters to $a = 0.02$, $b = 0.2$, $c = -65$ and $d = 8$. This type of neuron

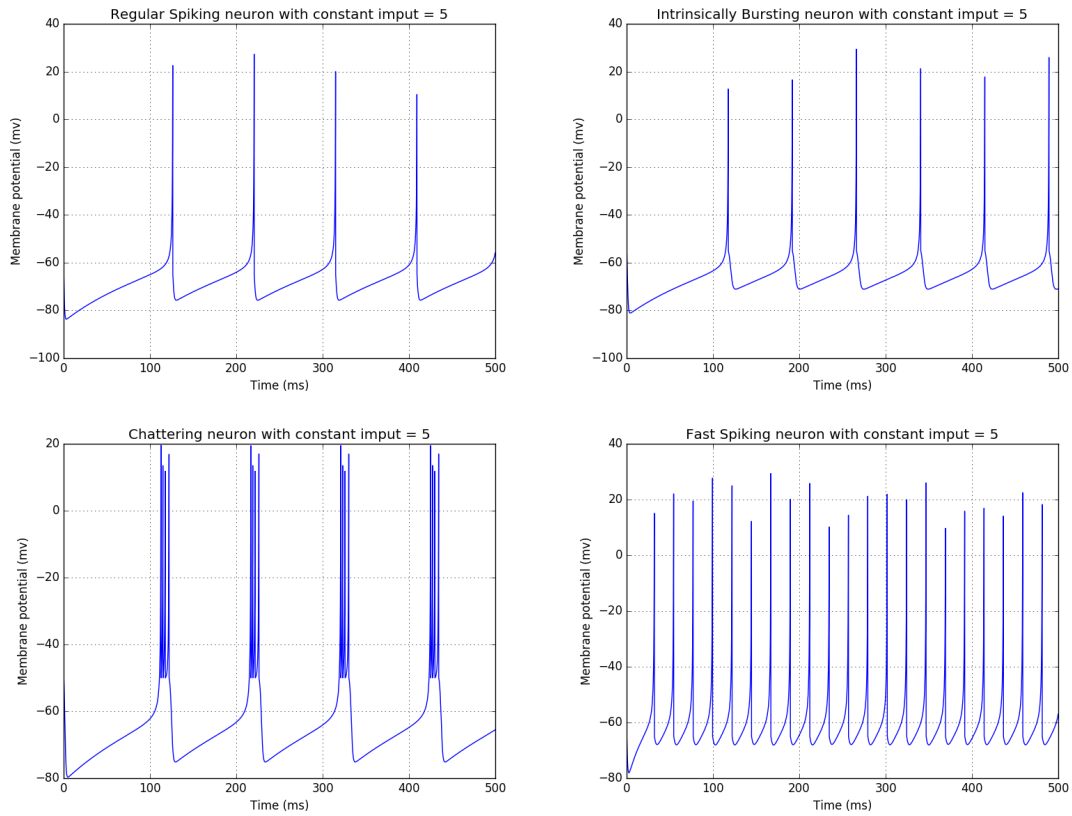


Figure 2.1: Types of neurons in the mammalian brain. Generated with the Brian Simulator [7] using the Izhikevich neuron model [6]

is the most common type of excitatory neuron in the brain. There is also a ratio of excitatory and inhibitory neurons of 4 to 1 in the mammalian brain, respectively [6].

In order to make use of the Izhikevich neuron model, Eq.2.3 is input to the Brian Simulator. This library computes the membrane potential voltage of the interacting neurons in the network and outputs all of their spiking times. This data will then be used to compute the NetRate algorithm.

2.3 Netrate

2.3.1 Diffusion processes

In order to infer the underlying structure of a network, [4] employed the NetRate algorithm developed by Rodriguez [5] by treating the network as a diffusion process.

The study of diffusion networks is based on the observation of the nodes in a system when they take a certain action: get infected by a virus, share a piece of information, etc. A problem concerning this kind of studies lies on the fact that we can only understand when and where these nodes propagate but not how or why they do so. An example of this is the propagation of a virus

in a population. We can tell who and when somebody got infected but not who infected him. For the rest of this section we will refer to the propagation of an infection as the object of study of the network.

To infer the mechanisms behind diffusion processes the time of infection is analysed. A model needs to be created with some assumptions about the structures that generate diffusion processes:

- The network in a diffusion process is fixed, unknown and directed: Connections do not change in time, it is not known what the connections are and connections are not bilateral.
- Infections are binary, they can only be infected or not infected, no partial infections are considered. For real neurons this means that there is either a spike or there is not.
- Infections across the edges of the network occur independently from one another. The probability of node i being infected by node j is not dependent on what the probability of node k infecting node i is.
- The likelihood of a node a infecting node b at time t is modelled by a probability distribution dependent on a, b and t .
- All infections in a network are observed during a recorded time window. This time frame is called horizon [5]. The larger the horizon, the higher the probability of more infections.

NetRate aims to describe how infections occur during a period of time in a fixed network. This is achieved by finding the optimal network and transmission rates that maximize the likelihood of a set of observed cascades to occur. The mathematical definitions that construct this model will be explained in the following section.

2.3.2 Mathematical definitions

The following definitions in this section are necessary for the construction of the model with which we intend to infer the connectivity of the network. First, the data that is going to be analysed will be defined:

Observations are carried out on a population of N nodes that have created a set of C cascades $\{\mathbf{t}^1, \dots, \mathbf{t}^{|C|}\}$. Each of the cascades \mathbf{t}^c contains the infection times of all the population within a time period T^c . Each of these cascades is an N -dimensional vector with recordings of when the nodes were infected in the cascade. If a node was not infected during the time period $[0, T^c]$, a symbol ∞ is assigned. This does not mean that the node never gets infected. For simplicity, we define $T^c = T$. Node i is parent of node j if $t_i < t_j$ within the cascade.

$$\mathbf{t}^c := (t_1^c, \dots, t_N^c), \quad t_k^c \in [0, T^c] \cup \infty \quad (2.6)$$

The pairwise interactions are to be studied in order to obtain the pairwise transmission likelihood between nodes in the network. It will be assumed that infections can occur at different rates along different edges in the network.

- $f(t_i|t_j, \alpha_{j,i})$ is the conditional likelihood of transmission between nodes j and i . It depends on the infection times (t_i, t_j) and pairwise transmission rate $\alpha_{j,i}$.
- A node cannot be infected by a healthy node. Node j , infected at t_j , can only infect node i at time t_i if and only if $t_j < t_i$.
- Transmission rate $\alpha_{j,i} \geq 0$.

The cumulative density function is defined as $F(t_i|t_j; \alpha_{j,i})$ and is obtained from the transmission likelihood. If a node j was infected at time t_j , the probability that node i is not infected by node j by time t_i is given by the survival function of the edge $j \rightarrow i$:

$$S(t_i|t_j; \alpha_{j,i}) = 1 - F(t_i|t_j; \alpha_{j,i}) \quad (2.7)$$

The instantaneous infection rate, or hazard function, of the edge $j \rightarrow i$ is the ratio of the transmission likelihood over the survival function as shown in Eq.2.8.

$$H(t_i|t_j; \alpha_{j,i}) = \frac{f(t_i|t_j; \alpha_{j,i})}{S(t_i|t_j; \alpha_{j,i})} \quad (2.8)$$

With a complete set of definitions, it will now be possible to derive the algorithm behind NetRate as it will be shown in the next section.

2.3.3 Derivation of NetRate

Rodriguez [5] derives NetRate by studying the individual probability of infection of the nodes and then building the whole of the network. The probability of survival of any cascade is the probability that a node is not infected until time T , given that the parents are infected at the beginning of the cascade. For a non-infected node i , the probability that any of the nodes $1 \dots N$ does not infect node i by time T is given by the product of the survival functions of each of the infected nodes k targeting node i because the different probabilities of infection are considered independent. This is illustrated in Eq.2.9.

$$\prod_{t_k \leq T} S(T | t_k; \alpha_{k,i}) \quad (2.9)$$

To compute the likelihood of a cascade $\mathbf{t} := (t_1, \dots, t_N | t_i \leq T)$ we require the the likelihood of the recorded infections $\mathbf{t}^{\leq T} = (t_1, \dots, t_N | t_i \leq T)$. Again, using independence, the likelihood factorizes as seen in 2.10. The likelihood of the cascade then becomes the conditional likelihood of the infection time given the rest of the cascade.

$$f(\mathbf{t}^{\leq T}; \mathbf{A}) = \prod_{t_i \leq T} f(t_i | t_1, \dots, t_N \setminus t_i; \mathbf{A}) \quad (2.10)$$

As in [19], a node gets infected when the first parent infects the node. We now compute the likelihood of a potential parent j of being the first one by using Eq.2.9.

$$f(t_i | t_j; \alpha_{j,i}) \times \prod_{j \neq k, t_k < t_i} S(t_i | t_k; \alpha_{k,i}) \quad (2.11)$$

In this step, we calculate the conditional likelihood of Eq.2.10 by adding all the likelihoods of the mutually disjoint likelihoods that each potential parent is the first parent:

$$f(t_i | t_1, \dots, t_N \setminus t_i; \mathbf{A}) = \sum_{j: t_j < t_i} f(t_i | t_j; \alpha_{j,i}) \times \prod_{j \neq k, t_k < t_i} S(t_i | t_k; \alpha_{k,i}) \quad (2.12)$$

Using Eq.2.10 and removing the condition $k \neq j$, the likelihood of infections then becomes:

$$f(\mathbf{t}^{\leq T}; \mathbf{A}) = \prod_{t_i \leq T} \prod_{k: t_k < t_i} S(t_i | t_k; \alpha_{k,i}) \times \sum_{j: t_j < t_i} \frac{f(t_i | t_j; \alpha_{j,i})}{S(t_i | t_j; \alpha_{j,i})} \quad (2.13)$$

However, Eq.2.13 needs to consider also the nodes that are not infected during the observation window. For this reason we add the multiplicative survival term from Eq.2.9 and replace the ratios from Eq.2.13 with hazard functions:

$$f(\mathbf{t}; \mathbf{A}) = \prod_{t_i \leq T} \prod_{t_m > T} S(T | t_i; \alpha_{i,m}) \times \prod_{k: t_k < t_i} S(t_i | t_k; \alpha_{k,i}) \sum_{j: t_j < t_i} H(t_i | t_j; \alpha_{j,i}) \quad (2.14)$$

The likelihood of a set of independent set of cascades $C = \{t^1, \dots, t^{|C|}\}$ is the product of the likelihoods of all the individual cascades given by Eq.2.14:

$$\prod_{\mathbf{t}^c \in C} f(\mathbf{t}^c; \mathbf{A}) \quad (2.15)$$

The goal of the algorithm is to find the transmission rates $\alpha_{j,i}$ of all the edges in the network such that the likelihood of the set of cascades is maximized.

$$\text{minimize}_{\mathbf{A}} - \sum_{c \in C} \log f(\mathbf{t}; \mathbf{A}) \quad (2.16a)$$

$$\text{subject to } \alpha_{j,i} \geq 0, i, j = 1, \dots, N, i \neq j, \quad (2.16b)$$

.

Here, $\mathbf{A} := \{\alpha_{j,i} \mid i, j = 1, \dots, n, i \neq j\}$ are the variables and the edges of the network are defined as the pairs of nodes whose transmission rates $\alpha_{i,j} > 0$.

The solution to Eq.2.16 found in [5] is given by Eq.2.17a. The survival and hazard functions are concave in the parameter(s) of the transmission likelihoods and, therefore, convexity of Eq.2.16 follows from linearity. The network inference problem from Eq.2.16 is thus convex for Power-Law,

Rayleigh and Exponential models of the likelihood function.

$$L(\{\mathbf{t}^1 \dots \mathbf{t}^{|C|}\}; \mathbf{A}) = \sum_c \Psi_1(\mathbf{t}^c; \mathbf{A}) + \Psi_2(\mathbf{t}^c; \mathbf{A}) + \Psi_3(\mathbf{t}^c; \mathbf{A}) \quad (2.17a)$$

$$\Psi_1(\mathbf{t}^c; \mathbf{A}) = \sum_{i:t_i \leq T} \sum_{t_m > T} \log S(T | t_i; \alpha_{i,m}) \quad (2.17b)$$

$$\Psi_2(\mathbf{t}^c; \mathbf{A}) = \sum_{i:t_i \leq T} \sum_{j:t_j < t_i} \log S(t_i | t_j; \alpha_{j,i}) \quad (2.17c)$$

$$\Psi_3(\mathbf{t}^c; \mathbf{A}) = \sum_{i:t_i \leq T} \log \left(\sum_{j:t_j < t_i} H(t_i | t_j; \alpha_{j,i}) \right) \quad (2.17d)$$

The terms in Eq.2.17a depend only on the infection time differences ($t_i - t_j$) and the transmission rates $\alpha_{j,i}$. Each of the terms adds a property to the solution of NetRate.

- The terms Ψ_1 and Ψ_2 apply a positively weighted norm on \mathbf{A} , thus encouraging sparse solutions.
- Ψ_2 penalizes the edges that transmit infections slowly and promotes edges that infect quickly.
- Ψ_1 penalizes edges to uninfected nodes until the time horizon. With a longer observation window the penalties become larger, but so does the probability of nodes becoming infected.
- Ψ_3 makes sure that all infected nodes have a minimum of one parent to avoid $\log 0 = -\infty$. Since the logarithm grows slowly, it slightly encourages infected nodes to have many parents.

2.3.4 Cascade generation

The maximization of the likelihood function requires data in the form of cascades in order to be computed. The time of infection of each of the nodes can be obtained from the network simulation but it must then be formatted into cascades. The rest of this section is based on [3], where cascade generation is explained.

1. At time $t = 0$, a random node is selected to carry the disease.
2. The disease propagates for a T amount of time (horizon) based on the pairwise transmission likelihood $f(t_i | t_j; \alpha_{j,i})$ of the edges in the network.
3. At the end of the simulation, a cascade is generated with the information from the times at which the nodes were infected.

As an example, let there be a network of 6 nodes ($N = 6$) and a horizon of $T = 20$. Let us select node 5 at time $t = 0$ to be the starting point of the experiment. The simulation begins and the disease spreads out. It infects node 2 at $t = 3$ and node 6 at $t = 5$. The resulting cascade has the form of Eq.2.6 would look like this:

$$\mathbf{t}^c = \{\infty, 3, \infty, \infty, 0, 5\} \quad (2.18)$$

Remember from Eq.2.6 that the symbol ∞ represents a node that is not infected during the cascade. Nodes 2 and 6 were infected while nodes 1, 3 and 4 remained healthy for the duration of the cascade. Since at time $t = 3$ the only infected node was 3, this node must have infected node 2. However, it becomes inconclusive as to which node infected 6 at time $t = 6$. We could be lead to believe that the uninfected nodes are not connected to any of the other infected nodes. However, cascades are probabilistic models and no one cascade can tell us what the values of $\alpha_{j,i}$ are. We would, therefore, require a large number of cascades in order to infer those values with a high confidence.

2.3.5 Performance metrics

Evaluating the performance of NetRate involves analysing the inferred network \hat{G} : which edges have been correctly inferred, which ones have been missed and what weights have been assigned to the inferred edges. These questions are answered in [5] by calculating the accuracy, precision, recall and MAE against the true network G^* :

1. Precision is the proportion of edges in the inferred network that exist in the true network.
2. Recall is the proportion of edges in the true network that exist in the inferred network.
3. Accuracy = $1 - \frac{\sum_{i,j} |I(\alpha_{i,j}^*) - I(\hat{\alpha}_{i,j})|}{\sum_{i,j} I(\alpha_{i,j}^*) + \sum_{i,j} I(\hat{\alpha}_{i,j})}$, where $I(\alpha) = 1$ if $\alpha > 0$ and $I(\alpha) = 0$, otherwise.
4. MAE = $E[|\alpha^* - \hat{\alpha}| / \alpha^*]$, where α^* and $\hat{\alpha}$ are the true and estimated transmission rates, respectively.

2.4 Biological Neural Network

2.4.1 Structure of the Network

In order to understand how neural networks are connected, a clear visual representation is required. This is achieved with an adjacency matrix plot. These matrices can be of three different types: binary ($\alpha_{i,j} \in \{0, 1\}$), ternary ($\alpha_{i,j} \in \{-1, 0, 1\}$) or real ($\alpha_{i,j} \in \mathbb{R}$). Due to the characteristics of biological neuron connections, real adjacency matrices are employed. In Fig.2.2 an adjacency matrix of a network of 20 nodes can be observed. When $\alpha_{j,i}^{BNN} \neq 0$, the target neuron i and the source neuron j are connected and a dot appears on the graph. The source nodes are indexed in the x-axis and the target nodes on the y-axis. The weight of each of the edges is represented by the diameter of the dot.

The superscript BNN in $\alpha_{j,i}^{BNN}$ is employed to differentiate between the weights in biological neural networks and the analogous transmission rates $\alpha_{j,i}$ in diffusion networks [3]. When neurons j and i are connected with a weight $\alpha_{j,i}^{BNN}$, everytime j spikes, it causes the membrane potential v from Eq.2.3 to increase by $\alpha_{j,i}^{BNN}$. If neuron i crosses the threshold of 30mV, it spikes. This phenomenon is proved in [4] and explained in section 2.4.2. Using the example in figure 2.2, when node 10 spikes, it causes nodes 13 and 9 to increase by $\alpha_{10,13}^{BNN}$ and $\alpha_{10,9}^{BNN}$, respectively.

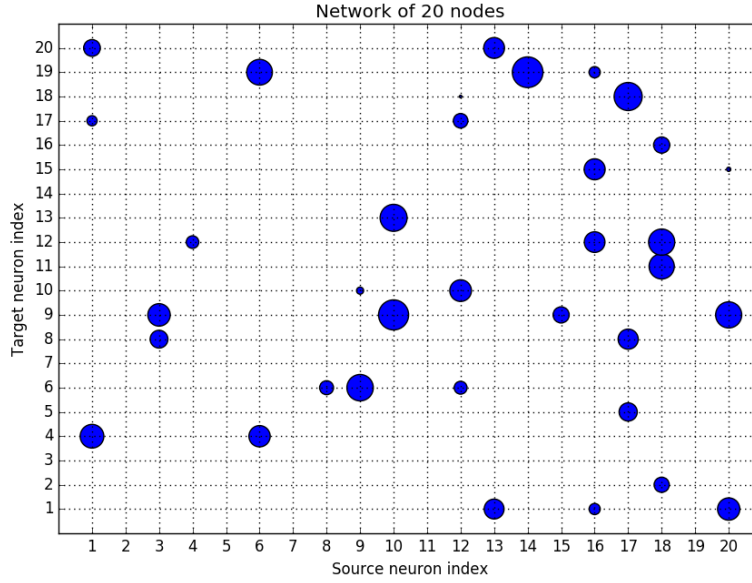


Figure 2.2: Adjacency matrix of a network of 20 nodes

The type of networks that were simulated in [4] are generated by Erdős & Reny random graphs, where each possible edge in the network has an independent probability p of being present. The weights assigned to the edges are the output of a uniform distribution in $(0,30]$, the threshold value in Eq.2.3. It can be observed that the adjacency matrix does not contain weights where $i = j$ because spikes do not increase the membrane potential of the source neuron.

2.4.2 Input stimulus model for cascade generation

The neurons in the brain are susceptible to input stimuli from the rest of the neurons in the network. This is represented in the Izhikevich neuron model with the I component in Eq.2.3. This term can be employed to model injected current in the form of a DC input or can be normally distributed¹ to represent noise from interactions with neurons that are outside the network being recorded.

The selection of an appropriate input stimulus for the neurons was a challenge encountered by Malhotra [4]. With a Gaussian input I , neurons spike at random times and there is no systematic way of selecting the beginning of a cascade. In a cascade where nodes 1, 3 and 5 spike in chronological order, each of them could have in turn their own cascade (i.e 1, 3 and 5; 3 and 5; and 5). However, this breaks the requirement of independence of cascades seen in section 2.3.1, where no same spike can appear in two cascades. For this reason, a well studied approach was required for the selection of cascades.

¹In the Izhikevich neuron model [6], the mean and standard deviation are equal to 0 and 5 for excitatory neurons and to 0 and 2 for inhibitory neurons, respectively.

The solution Malhotra found to this problem was to provide one neuron at a time with a constant input of 12mV and the rest of the neurons with Gaussian noise. This caused the selected neuron to spike periodically. With an appropriate selection of the DC input, the spiking frequency could be changed, and with a sufficiently long time between spikes, the network could settle into a steady state. Unlike infections in diffusion networks, neurons can spike more than once. For this reason the horizon was arbitrarily limited so as to not allow two spikes from the same cascade to occur in the same cascade and, therefore, obey the law of binary infections imposed by NetRate [4].

This method provides a systematic way of generating cascades: every time the node with DC input spiked, a new independent cascade was created. In order to obtain cascade information from all the nodes in the network, all nodes are stimulated over the course of an experiment. Otherwise, if only one node was selected, no information would be extracted from the nodes with no direct connection to it [3].

The experimental results obtained by Malhotra show that an optimal amount of spiking information that achieves a high inferring performance is achieved with a stimulation time of 4,000 ms. This is due to the underlying probabilistic nature of NetRate [3]. In other words, more data does not result in a higher performance.

2.4.3 Likelihood function

The ability of NetRate to infer the weights in the adjacency matrix \mathbf{A} stems from the fact that the shape of $f(t_i | t_j; a_{j,i})$ provides a probabilistic description of $\alpha_{j,i}$. The Izhikevich spiking neuron is modelled deterministically while the propagation of infections is probabilistic. For this reason the suitability of NetRate for the biological network inference was proved in [4].

As was explained in section 2.3.4, it is not possible to determine exactly which node caused some other node to become infected. However, this is not true for the Izhikevich neuron spikes. It was shown in [4] that the time it takes from a neuron i becoming unstable to the time it spikes is directly related to $\alpha_{j,i}$. A neuron becomes unstable when it crosses the threshold membrane value of 30mV. This can be caused by another neuron that spikes at that exact time or by random noise. In order to determine the shape that the likelihood function takes for different values of $\alpha_{j,i}$, an histogram of time was employed. It was observed that the likelihood function had an exponential and Rayleigh shape for low and large values of $\alpha_{j,i}$, respectively. Both of these distributions are convex for the solution of the optimization problem in Eq.2.16. NetRate only allows the use of one model, and because it is more relevant to infer the connections with larger weights, it was decided in [4] to employ the Rayleigh distribution.

	Accuracy	Recall	Precision	MAE
Average performance	0.667	0.633	0.704	0.997
Best performance	0.778	0.7	0.875	0.996
Worst performance	0.596	0.567	0.63	0.994

Table 2.1: Results for network inference obtained in [4]

2.4.4 Network inference results

The final test to determine the feasibility of the proposed algorithm in [4] was to compare an original simulated network and the resulting inferred network. Due to the underlying probabilistic nature of the network, the ability to infer the connections is different each time the experiment is performed. To provide a better representation of the performance of the algorithm, an average of 10 simulations was made. The results published in [4] can be seen in table 2.1.

When analyzing the results, it can be observed that the algorithm is good at detecting the edges with large weights from the network since it has a high value for accuracy, precision and recall. However, the high MAE shows that the algorithm is unable to infer the weights of the edges $\alpha_{j,i}$ correctly. A more extensive explanation for the high MAE can be found in [3].

Chapter 3

Improving the speed of NetRate

NetRate is a powerful algorithm that can make a good estimate of the connections of the nodes in a network. It analyses the spiking time of numerous neurons and constructs cascades that are used in the optimization problem. However, this is a computationally expensive process due to the large number of interactions between each of the neurons in the network. Moreover, as the size of the network increases, the number of cascades that are built grows exponentially. For a network of 10 neurons it only takes 8 minutes to obtain a result using one processor¹. However, for each addition of ten neurons to the system, the computation time increases threefold.

For this algorithm to eventually become useful in the area of neural signal processing it must be able to scale up and analyse systems of hundreds if not thousands of neurons. Fortunately, NetRate is an inherently parallel problem because it computes an independent optimization problem for each of the nodes of the network. A node j within a system of N nodes has $N - 1$ directed connections to all the neurons but itself. This makes the diagonal entries of the adjacency matrix equal to zero. Remember that the transmission rate of a node with itself is null $\alpha_{j,i} = 0$ if $j = i$.

A set of cascades is obtained from the spiking times of the system and assigned to the neuron node that originated them. This is necessary in order to compute each of the rows of the adjacency matrix. Then, they are used to build the components of the optimization problem. Therefore, after the cascade information is ready, each of the rows of the adjacency matrix can be computed with a different processor.

The objective function of NetRate's optimization problem makes use of logarithmic functions. Some solvers, such as SDPT3 [20, 21] (the one used by CVX) do not have support for these kind of problems and make use of recursive quadratic programming. This is a relatively new field of research [22] where a quadratic approximation of the objective function is taken. The solution to the new problem will converge to the one of the original problem for a sufficient number of iterations at which the initialization values are shifted towards the solution of the previous iteration.

¹The processors used throughout the whole work are the Intel(R) Core(TM) i7-4770 CPU @ 3.4GHz with 12GB of RAM

One of the problems encountered in [3] was the lack of parallelization capabilities of the CVX software package used for NetRate. The package was not built to be parallelized and, therefore, aiming to do so would require a low level redevelopment of the software. However, the attempts of speed up were always carried out from within MATLAB. For this reason, a new approach, where the parallelization is achieved by opening several MATLAB instances is presented.

3.0.1 Parallelization of NetRate

When an algorithm is parallelized and each of the processes are completely independent, all the information required for its computation must be available from the beginning. Otherwise, a special communication protocol between the processes must be carried out. Then, after all of them have finished, their outputs must be recombined in the same way as if only one processor had computed the whole algorithm. An analysis of the necessary steps for computing NetRate is critical to understand what benefit can be obtained from parallelization:

1. The two files obtained from the Brian Simulator containing the indexes and times of each of the spikes must be converted into cascades and assigned to each of the neurons in the network that originated them.
2. The components that constitute the objective function and the constraints are constructed for each of the nodes in the network. This requires the characterization of the hazard and log survival functions.
3. Each of these components is assembled together to form the optimization problem in 2.16 for each of the rows of the adjacency matrix.
4. The software package CVX is used to compute the optimization problem that returns the optimal weights.
5. Post-processing of the solution is carried out. This includes cutting off adjacency weights below a certain threshold in order to promote sparsity.

From the steps above, it can be observed that the one that requires the most amount of computation power is number 4, where CVX is executed. Moreover, the information required to compute each specific row of the adjacency matrix is obtained in step 2. Thus, the ramification of the jobs occurs from step 1 to 2. From this point onwards, the parallelization is possible. However, due to the insignificant computation time and an increased complexity of a parallelized step 2, it makes it unnecessary to parallelize. Steps 3 and 4 are very closely linked: in order to use CVX, the problem must be defined following the rules of CVX and, thus, it is easier if both of them are computed by the same processor.

It can be concluded that an optimal benefit from parallelization can be achieved by assigning the individual tasks corresponding to each of the rows of the adjacency matrix to the available number of processors. Let N be the number of nodes in a network, $\alpha_n = \{\alpha_{n,1}, \alpha_{n,2}, \dots, \alpha_{n,N}\}$

and let $C_n \subset C$, $n \in [1, N]$ be the set of cascades originated by node n . Then, the structure of the proposed parallelized NetRate is described in figure 3.1.

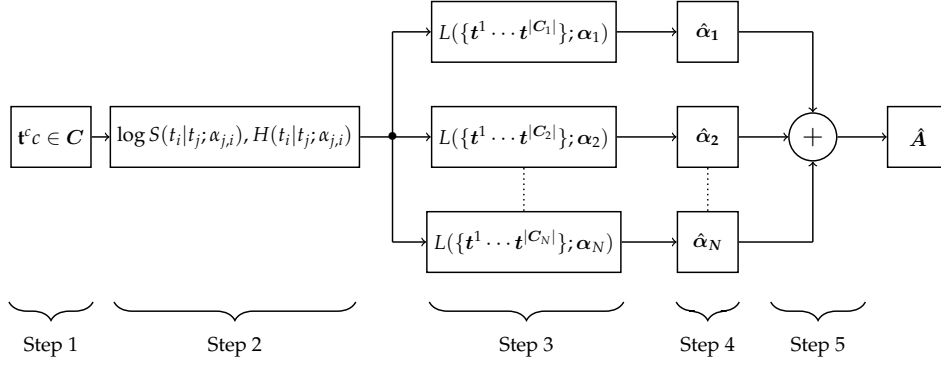


Figure 3.1: Diagram of the NetRate parallelization process

Originally, the algorithm computed steps 3 and 4 sequentially. Once the transmission rates of a row of the adjacency matrix were computed, it continued with the following one. However, in a parallelized NetRate, they are all computed at the same time with step 5 also involving the stacking of each of the $\hat{\alpha}_n$ vectors to form the matrix \hat{A} . The components in step 2 correspond to the ones seen in Eq.2.17a and whose solution is the assembled version of the one in step 3.

Once the structure of the algorithm is laid out, it still remains to plan how each of the jobs in steps 3 and 4 are will be assigned to the available processors. Not all the jobs take the same amount of time to be computed because they heavily depend on the number of cascades for their given node. As an illustration, a network of 10 neurons is simulated, and the number of cascades belonging to each node is shown in Eq.3.1.

$$NoC = \{12, 21, 62, 166, 21, 67, 17, 30, 18, 81\} \quad (3.1)$$

The mean of the distribution is 49 and the standard deviation 46. This means that the number of cascades differs significantly from node to node and that an appropriate way of distributing the jobs is required in order to keep all processors similarly busy. This is necessary because the whole algorithm will not finish until the last processor has estimated the weight parameters belonging to the last node.

Let M be the number of processors and N the number of nodes, where $N > M$. The first M with the largest number of cascades are assigned in order to each of the processors. Each of the

remaining $N - M$ nodes is assigned to the processors following Eq.3.2.

$$\operatorname{argmin}_n p_i + \operatorname{NoC}_n, \quad (3.2)$$

Where $i \in [0, M]$ is the processor number, $n \in [0, N - M]$ the node index and p_i is the sum of all the number of cascades assigned to processor i . This method ensures that each of the processors has as close number of nodes as possible. Using Eq.3.1 with $N = 10$, the distribution among $M = 4$ processors becomes:

$$p_1 = \{166\}, p_2 = \{81, 21, 12\}, p_3 = \{67, 21, 18\}, p_4 = \{62, 30, 17\} \quad (3.3)$$

The resulting number of cascades for each of the processors becomes 166, 114, 106 and 109, respectively. This is a more balanced distribution than if the nodes had been assigned in any other way.

It remains to clarify in which order each of the nodes must be computed. One constraint that limits the algorithm is memory. The larger the number of cascades that need to be computed, the more memory is required for the algorithm to compute the weights. The relationship between the number of cascades and size of the network is exponential and, as it grows, NetRate makes use of a larger amount of memory. Each of the processors requires its own memory to perform NetRate in parallel. Thus, it becomes prohibitive to use several processors at the same time for large networks. However, some minor adjustments can be made to increase the capability of a parallelized NetRate by choosing which nodes are computed first. If all the largest nodes are computed at the same time the computer will not be able to finish the task for a sufficiently big network. For this reason, half of the processors will start with the nodes whose number of cascades is the lowest. The other half will do the opposite and compute the ones with the highest number of cascades. This way, the number of cascades computed at any given moment is levelled out and the likelihood of sudden spikes of memory usage are reduced.

As mentioned above, the CVX package cannot be parallelized naturally. Since the previous attempts to do so failed [3], a new method had to be implemented. For this project, instead of parallelizing NetRate from within MATLAB, several MATLAB instances are opened that work independently of each other. Each of these instances outputs a csv file and they are all combined by a Python script at the end of the computation.

3.0.2 Speed improvement results

In this section the speed performance of the parallelized NetRate is evaluated. The computation time of NetRate for networks of different sizes, a stimulation period of 4000 ms and using 1, 4 and 8 processors is displayed in figure 3.2. Due to memory constraints of the computer, only up to 40 nodes were evaluated. As explained above, the more processors used at the time the more memory is required and this made the algorithm stall when using 8 processors in a network of 50

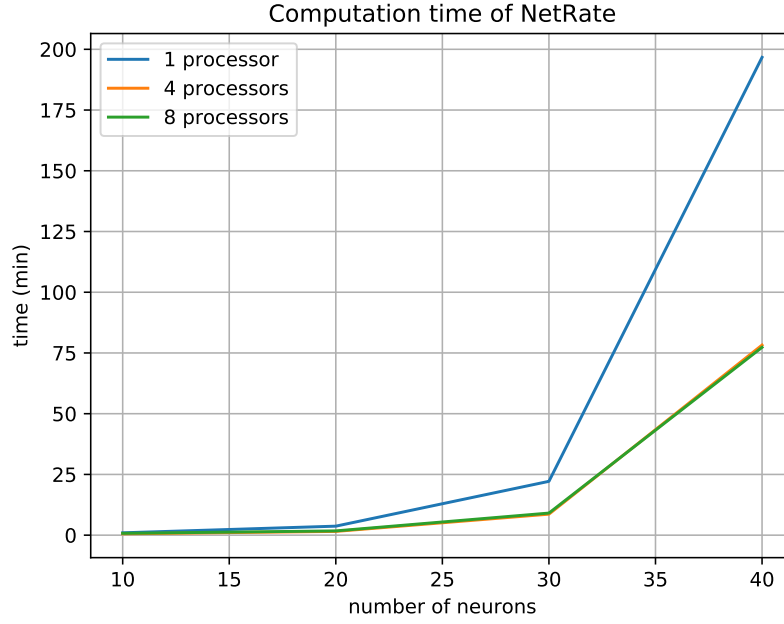


Figure 3.2: Computation time of NetRate

neurons.

There is a significant improvement in the speed of the algorithm when comparing 1 processor to 4 and 8 processors. For 30 neurons, it takes 22, 8 and 9 minutes for 1, 4 and 8 processors whereas for 40 neurons, it takes 196, 77 and 78 minutes. Although these are good results, they are far from ideal. Firstly, the time it takes to do the computation with 4 processors is not 4 times faster than with just one processor. It is, in fact, approximately 2.6 for the networks with 30 and 40 neurons. Moreover, using 8 processors instead of 4 results in no speed improvement for any of the networks. It is difficult to understand this behaviour because deeper analysis shows that all 8 processors are busy during the computation of the algorithm. One possible explanation is that the only steps that are actually being parallelized are number 3 from figure 3.1, where the optimization problem in 2.16 for each of the rows of the adjacency matrix is built, and half of step 4, where the CVX package is used but the solver has not been called. This means that the solver in the CVX package is a shared resource among all the running MATLAB instances and that each of the processors waits in a queue to compute its own row of the adjacency matrix. Further investigation into this hypothesis leads in this direction: when printing the progress of the optimization solver SDPT3, there is a linear behaviour i.e all processes print in an orderly fashion and there is no overlapping between them. However, further research into this issue must be carried out.

In this section it has been described what the steps of NetRate are, how the parallelization is implemented and what its limitations are. It is necessary to have a fast algorithm for it to be used with large networks. Finally, it was shown that although there is a significant improvement in the

speed of NetRate, it is not as good as desired, and it also poses further restrictions on memory usage.

Chapter 4

Simulating a biological neural network

Up until now the inference of networks using NetRate has been used only on simulations. A random structure was generated and the spikes simulated using the Brian simulator. This is very useful because it allows the possibility of comparing the inferred network to a ground truth and evaluating the performance of the algorithm. However, the goal is to be able to implement NetRate on real biological networks whose topology could provide insight to scientists. The analysis of real biological neural networks is met with many difficulties that need to be dealt with.

The main problem regarding the inference of the connectivity of a biological neural network is the lack of a ground truth with which to compare the capabilities of the algorithm. Although never to a full extent, there are certain ways that can help deal with this issue. The first is to simulate a network that replicates the characteristics of the real one. Under the assumption that the simulated network has a similar behaviour (not necessarily same connections) to the biological one, the algorithm can be implemented and tested. Then, the accuracy obtained can be taken to be an approximation to the accuracy inferred real network. However, this is a very big assumption and in reality the simulated network is very different to the real one. However, the main reason for testing on a simulated network is to verify that any change in the stimulation model of the system or any new method of cascade generation is still valid. A deeper explanation of this topic will be given in section 4.3.

Another way of measuring performance would be to separate the dataset into training and testing and running NetRate on the training set. With the resulting estimated weights, given that a set of neurons have fired at time t , estimate the neuron with highest probability of spiking. The relevance of this analysis stems from the fact that if $\alpha_{j,i}$ is high, then the probability of neuron i spiking given that neuron j has fired is also high. If the accuracy of prediction is sufficiently high, the network can be taken to be correctly inferred.

It is important to find a suitable dataset to analyse. It must either be made out of voltage

readings from an array of sensors in a cluster of neurons or spike times and indices¹. The second option is preferable because it would not require spike sorting. It would also be advantageous if the dataset contained some biological information as to the type of neurons present in the system, how they are connected (if there is any biological way of measuring it) or where they are located. This information would help in creating a reliable simulation of the system and having a way of estimating a ground truth. In the next section, the dataset that is going to be used will be discussed.

4.1 Mouse somatosensory cortex neuron dataset

For this project, the dataset that will be studied is the CRNCNS mouse somatosensory cortex SSC-3 dataset [8, 9, 10]. This is a recording of the spiking activity from a mouse's somatosensory cortex brain cells. These cells were grown in cultures for 2-4 weeks in vitro and 25 measurements of 1 hour were taken. The measurement method consisted of a 512 multi-electrode array that sensed the voltage in the culture for each of the neurons. These recordings were then spike sorted using PCA.

The somatosensory cortex is a set of modules located in the neocortex in the brain. The neocortex is vital in giving humans many of its cognitive abilities such as language processing, logic, sensory perception and many others. The neocortex shares many of its characteristics and architecture across different species of animals which makes it a very interesting subject of study. The somatosensory cortex is special because it is responsible for the touch sensations and because its anatomy and physiology has been intensively investigated [23].

The dataset consists of 25 different 1 hour recordings with a varying number of neurons ranging from 98 to 594. The average number of spikes per neuron for all datasets is 2.1 Hz and the sampling frequency is 20 kHz. The dataset also contains additional information on the x-y coordinates of each of the neurons in the cultures. With all this information, it is of interest to analyse what the distribution of spikes is. Neurons with larger connections will spike more often than the rest. Figure 4.1 displays how the spikes are distributed in the network. It is clear that the number of spikes per neuron follows an exponential distribution. Most of the neurons have sparse connections and will fire less than 6000 times during the length of the recordings while a few neurons will fire many times due to their high connectivity. In the next section, a simulated network will be implemented that tries to mimic the observable characteristics of the real 98 neuron network.

4.2 Input stimulus to the system

Previous work [4] simulated a network whose input was a DC voltage that stimulated each of the neurons one by one for a defined period of time (4 seconds). This proved to be very useful

¹Here, the index is the neuron number that generates a specific spike

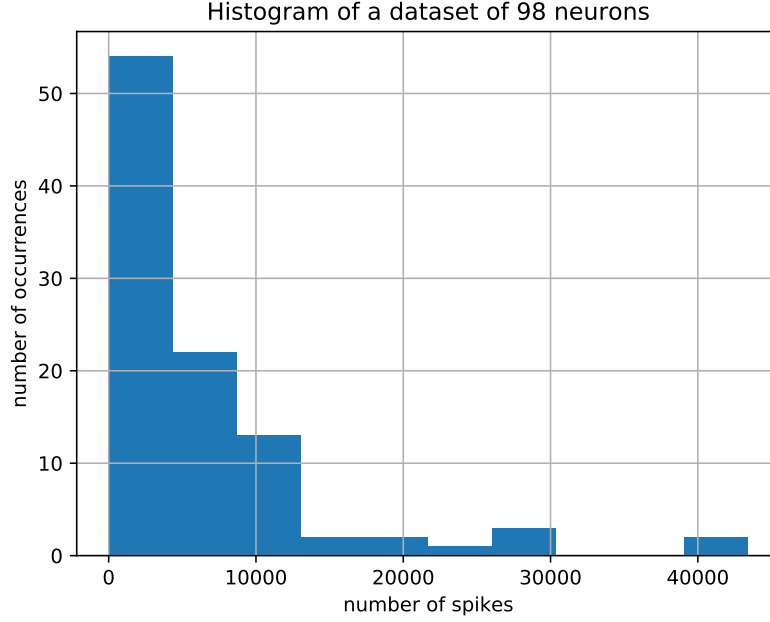


Figure 4.1: Histogram of the number of spikes in a network of 98 neurons

because it facilitated the analysis of each of the neurons regardless of their level of connectivity and because it provided a systematic way of generating cascades (more on this in section 4.4). However, the neural system cultures from the dataset are not stimulated. Instead, they are left alone to interact between each other. The neurons then communicate independently of the outside environment and spike at a lower frequency as a result.

The input stimulus cannot be left unchanged because the behaviour of the network would be radically different to that of the real one. It cannot be null either because then no interactions between the neurons would occur. Some type of random input noise must be present in order to have spikes. Moreover, the new model should have biological significance since a real network is being replicated. An option is investigated that could potentially meet these requirements.

4.2.1 System with random spikes

The proposed model intends to mimic biological behaviour by assuming that neurons spike when they want to transmit some information that they have conveyed by themselves. In order to do so, a random neuron is selected from the network and stimulated with random noise for some length of time.

The noise that is input to the selected neuron is taken from the absolute value of a normal distribution of zero mean and standard deviation equal to α^2 . Since, a model of only excitatory

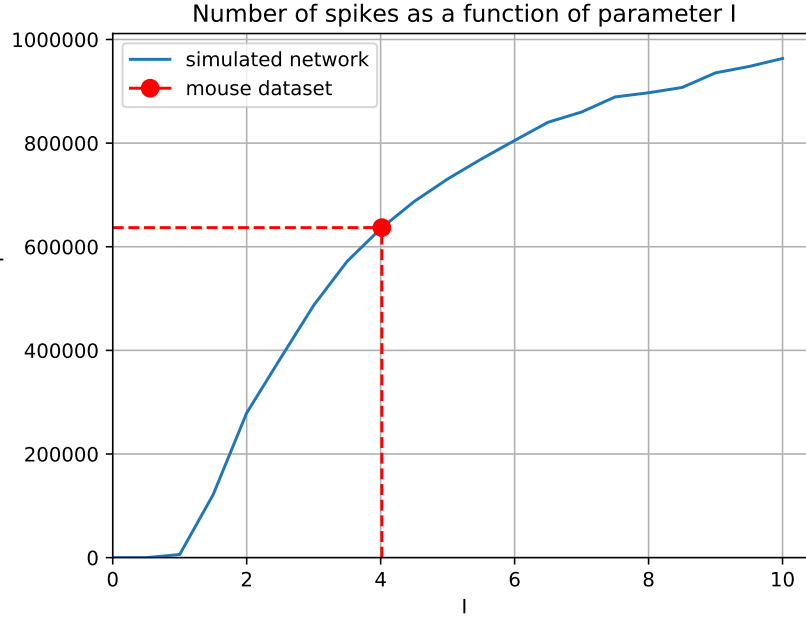


Figure 4.2: Number of spikes as a function of the parameter I for a 1 hour simulated network of 98 neurons and a random spike stimulus

neurons is being implemented, negative values from the distribution are not valid.

The amount of time the selected neuron is stimulated for is also random. It is taken from a uniform distribution in the range 0 to 200 ms. There is no evidence to support the selection of this number since to this day, the behaviour of the neuron is not very well understood. However, it must be sufficiently large for the neuron to spike but to not too big so as to allow other neurons to be stimulated too.

The benefit of this model arises from its ability to insure that every neuron has roughly the same probability of originating a spike train, from its random behaviour in the system and from its major biological resemblance than the model used in [4].

4.3 Number of spikes

At the beginning of this chapter the need for a simulated network that approximated the biological one was explained. Such a model can provide an approximation of performance of the algorithm. It is based on the assumption that the simulation is a faithful representation of the real nature of the network. Moreover, the differences between previous simulated networks and this new real network make it vital to verify that the algorithm would still work under these new conditions.

As seen in table 4.1, one of the most obvious changes with respect to previous simulations is the total number of spikes. This number is significantly smaller than before even though the

Type of network	Neurons	Duration	Number of spikes	Mean	Freq spikes/neuron
Real	98	3600 s	636878	6498.2	1.2 Hz
Sim. DC stimulus	98	392 s	4038313	41207.3	105.12 Hz

Table 4.1: Spike characteristics of different types of neural networks

observation time is larger. This is because the stimulation model forced the neurons to spike very frequently. In [4] the total observation time was equal to the defined length of stimulation multiplied by the number of neurons. Since the stimulation period was found to be optimal for 4 seconds, then for a network of 98 neurons, this would result in a total of 392 seconds of recordings. On the other hand, the real dataset consists of recordings of one hour. Therefore, the model of the simulation must be such that the number of spikes is roughly the same for a 1 hour simulation length.

4.4 Cascade generation

Once the network model is defined what remains to clarify is how the cascades will be built. The method used in [4] was simple and consistent. Since a DC stimulus was given to one neuron at a time, this neuron was selected to be the beginning of the cascade. This cascade would last for T length of time and only the first firing of each neuron would be taken into account. However, since the system no longer has a DC input, the cascade generation method must be changed. When selecting an appropriate method of cascade generation, certain factors are taken into account.

1. The higher the number of cascades that are generated, the more information will be conveyed and, in general, the better NetRate will be able to infer the connectivity of the network.
2. The more separated the cascades are from each other in the time domain, the more independent they will be. Cascade independence is a critical characteristic of high quality cascade because it maximizes the likelihood of the spikes in the time horizon being caused by a previous spike in the same cascade.
3. A high sparsity insures that enough cascade information is obtained from all the neurons in the network. Otherwise, only neurons who spike often will be the ones generating cascades.

4.4.1 Method of maximum cascades

4.4.2 Method of maximum independence

4.4.3 Optimal cascade generation

4.5 Concluding remarks

At the beginning of this chapter the need for a simulated network that approximated the biological one was explained. Such a model can provide an approximation of performance of the algorithm. It is based on the assumption that the simulation is a faithful representation of the real nature of the network. Moreover, the differences between previous simulated networks and this new real network make it vital to verify that the algorithm would still work under these new conditions.

Chapter 5

Inferring the connectivity of a mouse's neuronal system

5.1 Evaluating the performance without a ground truth

5.2 Results

Chapter 6

Conclusion

Bibliography

- [1] Kim T. E. Olde Dubbelink et al. “Disrupted brain network topology in Parkinson’s disease: a longitudinal magnetoencephalography study”. In: *Brain* 137.1 (2014), pp. 197–207. ISSN: 0006-8950.
- [2] S.C. Ponten, F. Bartolomei, and C.J. Stam. “Small-world networks and epilepsy: Graph theoretical analysis of intracerebrally recorded mesial temporal lobe seizures”. In: *Clinical Neurophysiology* 118.4 (2007), pp. 918–927. ISSN: 1388-2457. DOI: <https://doi.org/10.1016/j.clinph.2006.12.002>.
- [3] Pranav Malhotra. *Estimating the Topology of Networks from Distributed observations*. MEng FYP. Imperial College London, 2017.
- [4] Roxana Alexandru et al. “Estimating the Topology of Neural Networks from Distributed Observations”. In: *2018 26th European Signal Processing Conference (EUSIPCO)*. IEEE. 2018, pp. 420–424.
- [5] Manuel Gomez Rodriguez, David Balduzzi, and Bernhard Schölkopf. “Uncovering the temporal dynamics of diffusion networks”. In: *arXiv preprint arXiv:1105.0697* (2011).
- [6] Eugene M Izhikevich. “Simple model of spiking neurons”. In: *IEEE Transactions on neural networks* 14.6 (2003), pp. 1569–1572.
- [7] Dan Goodman and Romain Brette. “The Brian simulator”. In: *Frontiers in Neuroscience* 3 (2009), p. 26. ISSN: 1662-453X. DOI: 10.3389/neuro.01.026.2009.
- [8] Shinya Ito et al. “Spontaneous spiking activity of hundreds of neurons in mouse somatosensory cortex slice cultures recorded using a dense 512 electrode array. CRCNS. org”. In: *CRCNS. org* (2016).
- [9] Shinya Ito et al. “Large-scale, high-resolution multielectrode-array recording depicts functional network differences of cortical and hippocampal cultures”. In: *PloS one* 9.8 (2014), e105324.
- [10] AM Litke et al. “What does the eye tell the brain?: Development of a system for the large-scale recording of retinal output activity”. In: *IEEE Transactions on Nuclear Science* 51.4 (2004), pp. 1434–1440.
- [11] Barry Horwitz. “The elusive concept of brain connectivity”. In: *NeuroImage* 19.2 (2003), pp. 466–470. ISSN: 1053-8119. DOI: [https://doi.org/10.1016/S1053-8119\(03\)00112-5](https://doi.org/10.1016/S1053-8119(03)00112-5).

- [12] KJ Friston et al. "Functional connectivity: the principal-component analysis of large (PET) data sets". In: *Journal of Cerebral Blood Flow & Metabolism* 13.1 (1993), pp. 5–14.
- [13] Gert Pfurtscheller and Colin Andrew. "Event-related changes of band power and coherence: methodology and interpretation". In: *Journal of clinical neurophysiology* 16.6 (1999), p. 512.
- [14] Alan S Gevins et al. "Neurocognitive pattern analysis of a visuospatial task: Rapidly-shifting foci of evoked correlations between electrodes". In: *Psychophysiology* 22.1 (1985), pp. 32–43.
- [15] Alan L Hodgkin and Andrew F Huxley. "A quantitative description of membrane current and its application to conduction and excitation in nerve". In: *The Journal of physiology* 117.4 (1952), pp. 500–544.
- [16] Anthony N Burkitt. "A review of the integrate-and-fire neuron model: I. Homogeneous synaptic input". In: *Biological cybernetics* 95.1 (2006), pp. 1–19.
- [17] Barry W Connors and Michael J Gutnick. "Intrinsic firing patterns of diverse neocortical neurons". In: *Trends in neurosciences* 13.3 (1990), pp. 99–104.
- [18] Charles M Gray and David A McCormick. "Chattering cells: superficial pyramidal neurons contributing to the generation of synchronous oscillations in the visual cortex". In: *Science* 274.5284 (1996), pp. 109–113.
- [19] David Kempe, Jon Kleinberg, and Éva Tardos. "Maximizing the spread of influence through a social network". In: *Proceedings of the ninth ACM SIGKDD international conference on Knowledge discovery and data mining*. ACM. 2003, pp. 137–146.
- [20] Kim-Chuan Toh, Michael J Todd, and Reha H Tütüncü. "SDPT3—a MATLAB software package for semidefinite programming, version 1.3". In: *Optimization methods and software* 11.1-4 (1999), pp. 545–581.
- [21] Reha H Tütüncü, Kim-Chuan Toh, and Michael J Todd. "Solving semidefinite-quadratic-linear programs using SDPT3". In: *Mathematical programming* 95.2 (2003), pp. 189–217.
- [22] Michael JD Powell and Y Yuan. "A recursive quadratic programming algorithm that uses differentiable exact penalty functions". In: *Mathematical Programming* 35.3 (1986), pp. 265–278.
- [23] Henry Markram et al. "Reconstruction and simulation of neocortical microcircuitry". In: *Cell* 163.2 (2015), pp. 456–492.